Howard Huang

Seminar Report: Implementation of Photoacoustic Imaging on Ultrasound Systems

Seminar Paper: "The applicability of ultrasound dynamic receive beamformers to photoacoustic imaging."

Authors: Tyler Harrison, Roger J. Zemp

Overview: As mentioned in my project report, photoacoustic (PA) imaging is an imaging modality with a wide variety of medical uses including cancer detection (different tissues have different optical absorption), blood vessel visualization (hemoglobin has a strong PA signal), and instrument tracking (i.e. brachytherapy seed tracking). Currently, PA imaging requires additional hardware, even though US systems can already capture PA-derived signals (as they are sound waves). The seminar paper's authors attempted to resolve this problem by manipulating the speed of sound parameter in conventional US beamforming. Since the main goal of our project is to develop real-time PA imaging on an US system, this paper presents an alternative approach to PA imaging that we can compare against our own approach.

Summary of Paper's Method (Overall Theory):

The main issue that prevents US systems from correctly processing PA signals is the difference in beamforming for PA vs US signals. As shown in the diagram below, general delay-and-sum beamforming for PA and US signals requires knowledge of the time delays needed to align signal data captured from each transducer element in order to get an RF signal corresponding to a particular focal point. US signals are double-trip (they travel to and from the US transducer) while PA signals are single trip. The difference in travel times results in different beamforming equations for each type of signal.

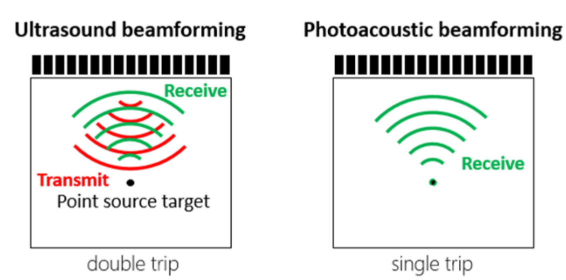

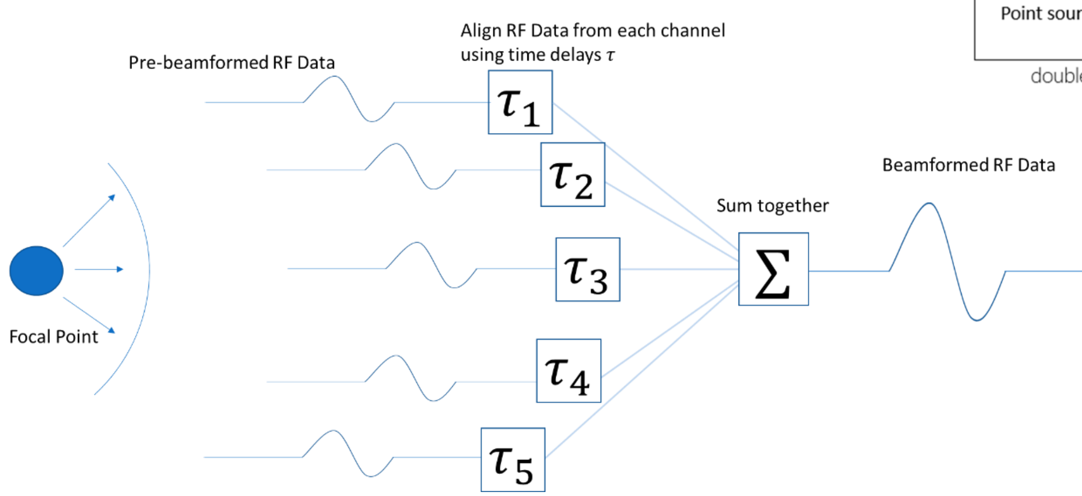

Figure above demonstrating difference in US/PA travel times (provided by my mentor, Kai).

Figure on left summarizing main components of beamforming (made by me).

The main equation relating the distance R from focal image point to center of an US image reconstruction line is $R = ct/2$, where R is distance, c is speed of sound wave, and t is travel time. Observe that t is divided by 2 for an US signal since the sound wave travels twice (double trip). The formula describing time delay for signals from an image point is:

$$t_n(R, x_n, \theta) = \frac{\sqrt{(x_n - R\sin\theta)^2 + R^2\cos^2\theta}}{c}$$

Where *R* is distance from image point to center of reconstruction, *x* is lateral distance of transducer element to reconstruction center, and theta is steering angle of the reconstruction line. For lateral scanning, reconstructed image lines are perpendicular to the transducer, resulting in varying *x* values and constant steering angle of 0. For sector scanning (yielding the common 'fan' shaped US images), all reconstructions share the same center so *x* is constant while the steering angles are varying.

When we apply a second order approximation for the US time delay equation we get:

$$\underbrace{\tau_n(t, x_n, \theta)}_{\text{Travel time for element n}} = -\underbrace{\frac{x_n \sin\theta}{c}}_{\text{"Steering" Term}} + \underbrace{\frac{x_n^2 \cos^2\theta}{c^2 t}}_{\text{"Refocusing" Term}} \quad \text{US Time Delay Equation}$$

Observe that the left "steering" term is only dependent on orientation of reconstruction line (steering angle and lateral distance to center), while the right "refocusing" term is also dependent on the travel time of the signal.

For PA beamforming, the time delay is for single trip signals, resulting a distance relation of $R = ct$ and an approximate time delay of:

$$\tau_n(t, x_n, \theta) = -\frac{x_n \sin\theta}{c} + \frac{x_n^2 \cos^2\theta}{2c^2 t} \quad \text{PA Time Delay Equation}$$

Direct manipulation of these time delays is not possible on most US systems, however some systems do allow for the adjustment of the speed of sound parameter $c = a * c\_0$, where a is an changeable scaling factor. By setting $a = \sqrt{2}$, we can effectively "convert" the US beamforming equation into the PA beamforming equation (modify the time delay equation shown above from US to PA time delays) to allow for proper PA imaging.

<u>Experimental Setup: (Overall outline in the diagram below)</u>

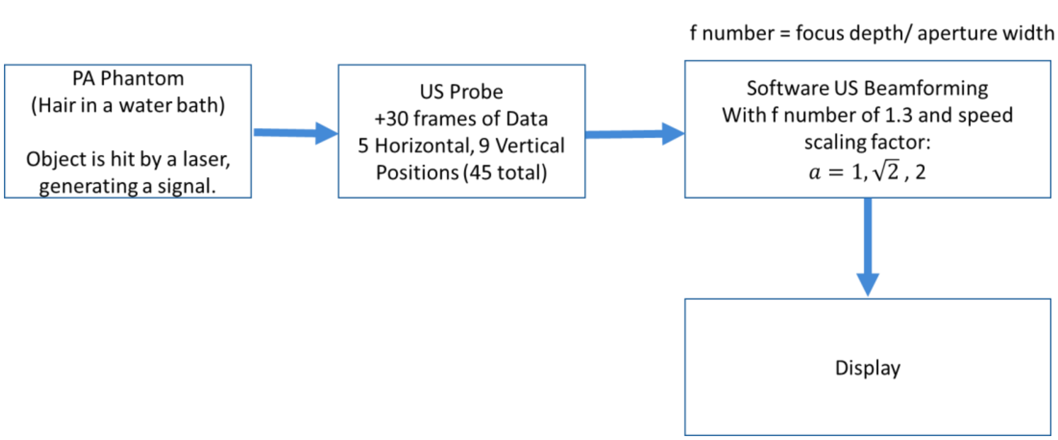

To test their beamforming modification, the authors of the paper used linear and sector scanning US probes on a PA phantom at 45 different positions with a PA-scaled f number of 1.3 (f number is ratio of focus depth against aperture width, greater f numbers correspond to greater focus depths and higher resolution images. The authors scaled the US f number by a/2 to set the f number to 1.3 for the PA image). The PA phantom was a human hair suspended in a water bath, with PA signals generated by firing a 700 nm laser at the hair. To test lateral resolution, the authors centered the hair against the US probe at different depths. Most importantly, the authors <u>set the speed scaling factor for the US beamformer at 3 different settings: $a = 1, \sqrt{2}, 2$</u>, with the prediction that the setting $a = \sqrt{2}$ produces the best resolution images (as it 'corrects' the US beamforming algorithm for PA signals).

<u>Results:</u>

Below are the results of the reconfigured US lateral and sector scan images.

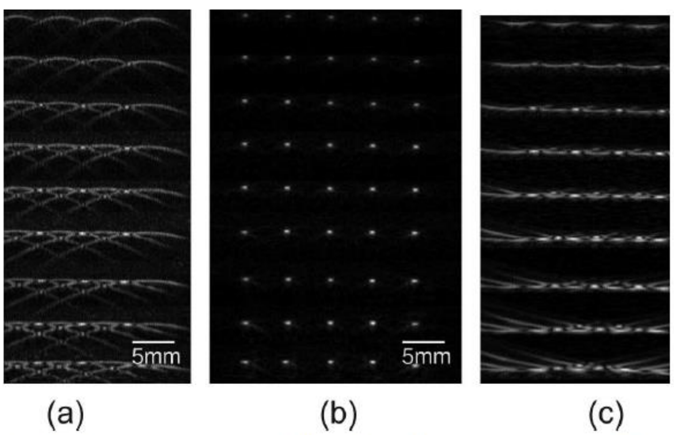

Fig. 3. Composite ultrasonically-beamformed linear-scanned images from experimental data with (a) $a = 1$, (b) $a = \sqrt{2}$ (identical to PA beamformer), and (c) $a = 2$.

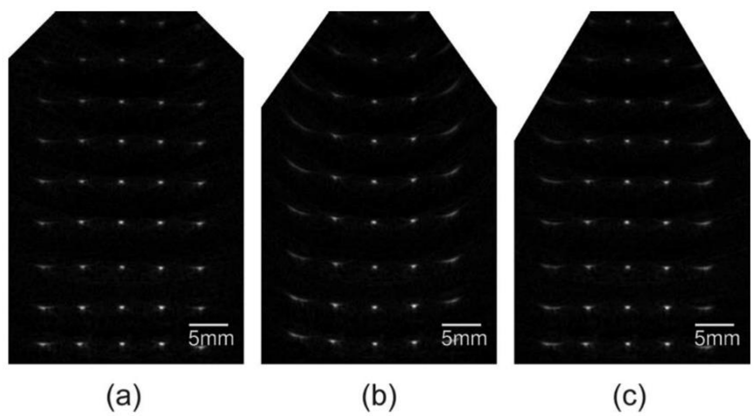

Fig. 4. Composite sector-scanned images using (a) PA beamforming and scaled-c US beamformer with $a = \sqrt{2}$ using (b) simple depth scaling, and (c) coordinate re-mapping.

In the linear scanning results, the image with the clearest resolution was obtained using the speed scaling of $a = \sqrt{2}$. For sector scanning results, only the $a = \sqrt{2}$ option is shown (with additional depth and polar coordinate image warping to reduce distortion). In terms of lateral resolution, the authors stated that results were improved by a factor of at least 8 from the default speed setting ($a = \sqrt{2}$), with improvements more noticeable at greater depths (i.e. at 5 cm for a centered signal, the optimal setting displays the signal centered at 0.61 ± 0.006mm while the default beamforming displays it around 17.4 ± 0.3mm with significant visual distortions). For sector scanning, the authors mention that additional polar coordinate rewarping of the image was needed to correct for visual distortions. The steering term was not resolved by the parameter modifications and is nonzero in sector scanning, creating distortions in the PA image. For both images the depth scaling is off by a factor of $1/\sqrt{2}$ but was corrected with a simple rescaling of image depth.

Analysis:

The main significance behind the author's findings is that the implementation of real-time PA imaging on US systems is possible. A simple adjustment of an US beamformer's parameters (scale signal speed by a factor of $\sqrt{2}$) results in reasonably accurate PA images for linear scanning. The paper's methods also demonstrate clear flaws that illustrate the need for improved PA imaging methods on US systems (i.e. our project). Ultimately, the adjustment of parameters does not resolve all issues of US to PA beamforming, as both the image depth and steering angle terms were incorrect and produced noticeable distortions in the sector scan image (requiring additional image rewarping for certain US probes limits this approach's flexibility). Most importantly, the ability to adjust the speed of sound parameter might not exist on all US systems. Overall, since this paper only did a demonstration using 2 US probes on a very basic PA phantom, it would be interesting (and informative) to see what other PA phantom and US probe setups would work using their PA imaging method. As future work, the paper's authors may also want to consider manipulating other US imaging parameters besides speed of sound in order to determine further possible refinements that can result in more accurate PA imaging on US systems. Finally, the results from the paper present a relevant base for comparisons against our own project (in terms of accuracy/image resolution, flexibility, ease of use/implementation) since we intend to develop a PA imaging method for US systems as well.

Conclusion:

Overall, the authors of the paper demonstrated a simple method to allow certain US systems (those that provide manipulation of the speed of sound parameter in beamforming) to display PA signal data properly. We hope to replicate their successes in our own PA imaging approach, and provide another viable implementation for PA imaging. Since our approach focuses on rebeamforming RF data (which can be provided from many US system), we hope to achieve a system that can be deployed on more US systems and is perhaps simpler to use, since we would create a software framework that processes the PA image automatically, instead of having users modify the US beamformer and image settings themselves.

References:

Harrison, Travis, and Roger J. Zemp. "The applicability of ultrasound dynamic receive beamformers to photoacoustic imaging." *Ultrasonics, Ferroelectrics, and Frequency Control, IEEE Transactions on* 58.10 (2011): 2259-2263.

Beamforming diagrams (on the first page) are provided by me and my mentor kai. Experimental outline diagram was also made by me. PA results from referenced seminar paper.